INTERNATIONAL JOURNAL OF CLIMATOLOGY
Int. J. Climatol. **37**: 4938–4948 (2017)
Published online 19 May 2017 in Wiley Online Library
(wileyonlinelibrary.com) DOI: 10.1002/joc.5134

RMetS
Royal Meteorological Society

Onset of the Bay of Bengal summer monsoon and the seasonal timing of ENSO's decay phase

Shuyue Sun,[a,b] Rongcai Ren[a,c]* and Guoxiong Wu[a]

[a] *State Key Laboratory of Numerical Modeling for Atmospheric Sciences and Geophysical Fluid Dynamics (LASG), Institute of Atmospheric Physics, Chinese Academy of Sciences, Beijing, China*

[b] *College of Earth Sciences, University of Chinese Academy of Sciences, Beijing, China*

[c] *Collaborative Innovation Center on Forecast and Evaluation of Meteorological Disasters and KLME, Nanjing University of Information Science and Technology, China*

ABSTRACT: Based on multiple sources of atmospheric and oceanic data, this study demonstrates a close relationship between the onset of the Bay of Bengal (BOB) summer monsoon (BOBSM) and the seasonal timing of El Niño–Southern Oscillation (ENSO)'s decay phase. Through distinguishing 'later-decay' and 'normal-decay' ENSO events, it is found that a later/earlier onset of the BOBSM following El Niño/La Niña is mainly caused by later-decay ENSO events, while no significant changes in BOBSM onset can be identified between normal-decay El Niño and normal-decay La Niña events. Diagnosis of the related dynamic and thermodynamic processes further confirms that, for later-decay ENSO events that remain active until mid-April, persistent ENSO-induced 'atmospheric-bridge' processes can yield a stronger vertical coupling of circulation between the upper and lower troposphere, and thus an anomalously earlier (later) BOBSM onset following a later-decay La Niña (El Niño). In the lower troposphere, the persisting zonal sea surface temperature (SST) gradient between the Indian Ocean and the western Pacific following later-decay ENSO events can significantly modulate the lower tropospheric barotropic instability over the northern BOB, which in turn overwhelms the local SST conditions to dominate the development of monsoon convections. In the upper troposphere, later-decay ENSO alters the position of the South Asian high and the upper atmospheric divergence-pumping through the anomalous Walker circulation. In contrast, due to the earlier damping of normal-decay ENSO, the BOBSM onset processes are barely modulated.

KEY WORDS Bay of Bengal; summer monsoon onset; seasonal timing of ENSO's decay phase

Received 2 January 2017; Revised 15 March 2017; Accepted 17 April 2017

1. Introduction

The onset of the Asian Summer Monsoon (ASM), as an important indicator of the seasonal transition from winter to summer in the Northern Hemisphere, is often accompanied by radical changes of regional circulation and followed by frequent occurrence of summer droughts and floods in Asia and China (Tao and Chen, 1987; Chen *et al.*, 1991; Liu and Ding, 2008). The onset of the ASM has been divided into three successive stages (Wu and Zhang, 1998; Wang and LinHo, 2002; Mao *et al.*, 2003), including the onset of the Bay of Bengal summer monsoon (BOBSM, occurs in late April), the onset of the South China Sea summer monsoon (SCSSM, in mid to late May) and the onset of the Indian summer monsoon (ISM, in early June). These onset phenomena are closely connected through a series of dynamic and thermodynamic processes (Lau and Yang, 1997; Webster *et al.*, 1998; Wu and Zhang, 1998; Wang and LinHo, 2002; Mao *et al.*, 2003; Liu *et al.*, 2015a). In particular, after its onset, the BOBSM extends eastwards to the South China Sea (SCS) and western Pacific, and can be a trigger for the onset of the SCSSM (Lau and Yang, 1997; Webster *et al.*, 1998; Wang and LinHo, 2002). However, the westward extension of the BOBSM is trapped because of the Gill-type circulation response to the convective latent heating of the BOBSM, which is referred to as 'the monsoon onset barrier' (Wu and Zhang, 1998; Yan, 2005; Liu *et al.*, 2015a). As the earliest stage of the ASM, the onset date of the BOBSM exhibits large interannual variabilities. Tropical sea surface temperature (SST) anomalies associated with the El Niño–Southern Oscillation (ENSO) in the tropical central-eastern Pacific has been found to have a significant correlation with the onset date of the BOBSM (Joseph *et al.*, 1994; Ju and Slingo, 1995; Chao and Chen, 2001; Mao and Wu, 2007; Liu *et al.*, 2015b). Specifically, the BOBSM onset process is significantly postponed/advanced in warm/cold ENSO-decay years. Based on a series of composite analyses of BOBSM onset against ENSO indices, Liu *et al.* (2015b) indicated that a later/earlier onset of the BOBSM is mainly due to the effective modulation of ENSO on the local vertical coupling of the tropospheric circulation over the BOB region. Specifically, ENSO acts to alter the atmospheric barotropic instability and affect the formation of BOBSM onset convection by inducing an anomalous zonal SST

* Correspondence to: R. Ren, LASG, Institute of Atmospheric Physics, CAS, P.O. Box 9804, Beijing 100029, China. E-mail: rrc@lasg.iap.ac.cn

© 2017 Royal Meteorological Society

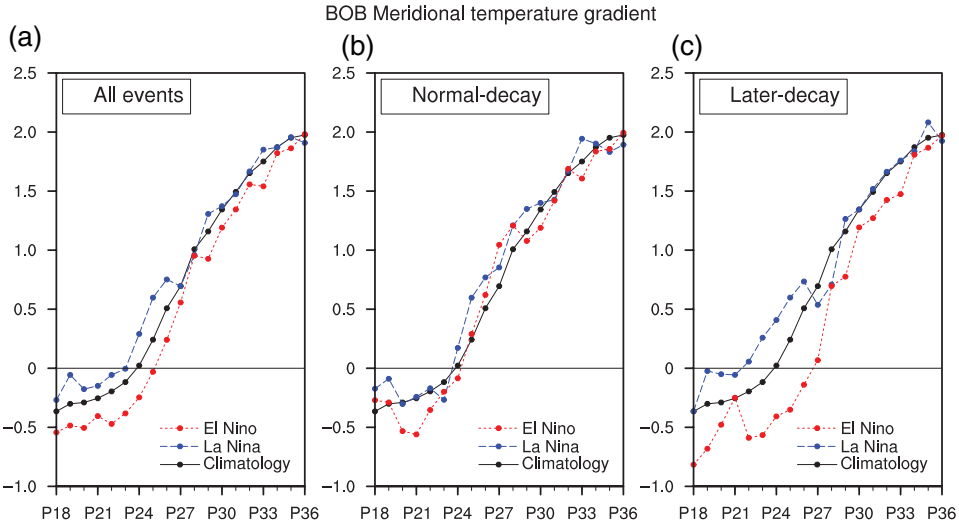

Figure 1. Composite pentad evolutions of the area-mean meridional temperature gradient in the upper troposphere (200–500 hPa) over the eastern BOB (5°–15°N, 90°–100°E) in ENSO-decay years for (a) all, (b) normal-decay and (c) later-decay ENSO events that are moderately strong. Black, blue and red curves represent the climatology and the composites for cold and warm ENSO events, respectively.

gradient in the lower troposphere over the Indo-Pacific region. In the upper troposphere, the meridional location of the South Asian high (SAH) and the associated dynamical divergence-pumping effect of the SAH over the BOB region can be modulated by the ENSO-induced convection anomalies over the southern Philippines.

It is known that ENSO exerts its remote influences on the Indo-Pacific region through a series of ENSO-induced 'atmospheric-bridge' processes, including anomalous Walker circulation, cloud–radiation feedback processes, wind–evaporation–SST feedback processes and oceanic dynamic processes (Julian and Chervin, 1978; Lau and Nath, 1996; Oort and Yienger, 1996; Masumoto and Meyers, 1998; Alexander *et al.*, 2002; Ren *et al.*, 2016). An important feature that demonstrates ENSO's remote effects is the significant SST anomalies over the Indian Ocean basin (IOB) and the Indo-Pacific region in the spring of ENSO-decay years (Klein *et al.*, 1999; Alexander *et al.*, 2002; Huang and Kinter, 2002; Xie *et al.*, 2002; Lau and Nath, 2003; Tokinaga and Tanimoto, 2004; Yu *et al.*, 2005; Li *et al.*, 2012), which may act as a mediator for ENSO's influences on the ASM and the climate anomalies over Asia (Xie *et al.*, 2009). Actually, many previous studies, including those listed above, have proved the crucial role played by the IOB or the Indo-Pacific ocean in passing ENSO's effects from the tropical eastern Pacific to the South Asia region (Lau and Nath, 2000, 2012; Wang *et al.*, 2000; Annamalai *et al.*, 2005; Yoo *et al.*, 2006; Yang *et al.*, 2007; Li *et al.*, 2008; Yuan *et al.*, 2008). However, due to the multi-timescale variabilities of ENSO and the complexity of the influencing processes, large uncertainties still exist with respect to the relationship between ENSO and the ASM systems. For example, some warm/cold ENSO events are not followed by a significantly later/earlier onset of the BOBSM, or the changes in monsoon onset between warm and cold ENSO years are sometimes less significant (Liu *et al.*, 2015b) (also as shown in Figure 1). Further investigation of the remote effects of ENSO on the ASM system is obviously still needed.

Table 1. List of the decay years for moderately strong ENSO events since the 1940s.

El Niño	1952, 1958, 1964, 1966, 1970, 1973, 1977, **1983**, **1987**, 1988, **1992**, 1995, **1998**, 2003, 2007, **2010**
La Niña	**1950**, **1955**, **1956**, 1957, 1965, **1968**, **1971**, 1972, **1974**, 1976, **1985**, **1989**, **1996**, 1997, **1999**, 2000, 2006, 2008, 2011, 2012

Bold typeface indicates later-decay ENSO events.

By focusing on the interannual and interdecadal variabilities of the ENSO–IOB relationship, Ren *et al.* (2016) and Li *et al.* (2012) demonstrated significantly enhanced and prolonged effects of ENSO on the IOB for those ENSO events that decay far more slowly. They showed that the warm/cold SST anomalies over the IOB that usually occur in the spring of ENSO-decay years can remain significant till summer for later-decay ENSO events. By distinguishing between later-decay and normal-decay events in the past 70 years, Ren *et al.* (2016) further indicated that the ENSO-induced 'atmospheric-bridge' processes, except the surface wind–evaporation feedback process, can extend from spring to summer and continue to affect the IOB and Indo-Pacific until the summer in later-decay ENSO years. The main objective of this study is to examine whether a later or earlier seasonal timing of ENSO's decay phase is a crucial factor for the significant effects of ENSO on the onset of the BOBSM. To achieve this, we first follow Ren *et al.* (2016) to categorize the moderately strong ENSO events into the normal-decay and the later-decay types based on their seasonal evolutions. We then examine the possible contrast of BOBSM

© 2017 Royal Meteorological Society

onset between normal-decay and later-decay ENSO types, and diagnose the differences in the related dynamic and thermodynamic processes during BOBSM onset between normal-decay and later-decay ENSO, including surface air–sea interactions and the atmospheric circulation in the lower and upper troposphere. We expect the results to show that it is those later-decay ENSO events that have dominated the remote relationship between ENSO and the BOBSM onset. In a companion paper in the future, we further expect to show that later-decay ENSO events have also dominated ENSO's influences on the ISM onset.

The rest of the article is organized as follows. Section 2 describes the data and methodology. Section 3 investigates the dominance of later-decay ENSO events in the ENSO–BOBSM relationship. Section 4 further examines the contrast in the dynamic and thermodynamic processes of BOBSM onset between later-decay and normal-decay ENSO events. A discussion and conclusions are presented in Section 5.

2. Data and method

2.1. Data

To describe the characteristics of BOBSM onset, we extract daily surface and atmospheric variables including air temperature, the 3-D wind field, sea level pressure and surface skin temperature, with a horizontal resolution of $1.25^\circ \times 1.25^\circ$ and 37 vertical pressure levels ranging from 1000 hPa to 1 hPa, from the Japanese 55-year Reanalysis (JRA-55) dataset for the period 1958–2014 (Kobayashi *et al.*, 2015). To distinguish later-decay from normal-decay ENSO events and to maintain data consistency, monthly SST records with a horizontal resolution of $1^\circ \times 1^\circ$ from 1985 to 2014 are derived from the Japan Meteorological Agency's Centennial in situ Observation-Based Estimates (COBE) of the SST fields (Ishii *et al.*, 2005), which has been used as the input for JRA-55 since 1958. To obtain the monthly anomalies of all variables, we remove the climatological annual cycle from the original fields.

The European Center for Medium-Range Weather Forecasts interim reanalysis dataset (ERA-Interim; Dee *et al.*, 2011) from 1979 to 2013, and the Hadley Centre Sea Ice and Sea Surface Temperature dataset (HadISST; Rayner *et al.*, 2003), are also adopted to validate the results from JRA-55 (not shown).

2.2. Method

2.2.1. Definition of BOBSM onset

In the Asian tropics and subtropics, seasonal transition of the circulation patterns from winter to summer can be represented effectively by a southward-to-northward inversion of the tilting direction of the vertical ridge surface of the subtropical high (Mao, 2001; Mao *et al.*, 2004). Accordingly, Mao and Wu (2007) proposed an BOBSM onset index based on the area-averaged meridional temperature gradient (MTG) near the vertical ridge surface of the subtropical high in the upper troposphere. They further justified that the MTG index can capture the essential features of BOBSM, and represent the interannual variabilities of its onset more effectively, compared with other monsoon onset indices based on 850 hPa zonal wind, or outgoing longwave radiation (OLR). In this study, we follow Mao and Wu (2007) and define the BOBSM onset date as the day of the seasonal reversal (i.e. $\mathrm{d}T/\mathrm{d}y = 0$) of MTG. Specifically, the onset date of the BOBSM is defined as the date when the area-averaged upper tropospheric (200–500 hPa) MTG over the eastern BOB (5°–15°N, 90°–100°E) changes from negative to positive and remains positive for more than 10 days (Mao *et al.*, 2004; Mao and Wu, 2007; Liu *et al.*, 2015b). We also verify that this MTG-defined onset date is highly consistent with that defined based on other indices, including the one using a threshold value of 0 $\mathrm{m\,s^{-1}}$ for the area-averaged 850-hPa zonal wind (Wang *et al.*, 2004, 2009) and the one using a threshold value of 230 $\mathrm{W\,m^{-2}}$ for OLR (Ananthakrishnan and Soman, 1989; Wang and Wu, 1997) (not shown). They all imply the establishment of the key lower-level westerlies and deep convection over the BOB monsoon region.

2.2.2. Definition of later-decay and normal-decay ENSO events

As in Li *et al.* (2012) and Ren *et al.* (2016), we use the area-mean SST anomalies in the Niño3 region (i.e. the Niño3 index) to represent the ENSO signal. To suppress the possible impacts of the long-term SST warming trend on our results, we produce a detrended SST timeseries before our analysis. Following Ren *et al.* (2016), we objectively identify each of the moderately strong warm/cold ENSO events (November–December–January mean Niño3 index exceeding 0.7 standard deviations) since the 1940s, as a later-decay event when its Niño3 amplitude in April is above the averages of all warm/cold ENSO events. Otherwise, it is categorized as a normal-decay event (see Table 1, in terms of ENSO-decay years). The remarkably contrasting seasonal evolutions of the tropical SST anomalies in ENSO-decay years between normal-decay and later-decay ENSO events are presented in Ren *et al.* (2016).

3. Dominance of later-decay ENSO events in the ENSO–BOBSM relationship

Figure 1 displays the composite pentad evolutions of the area-mean MTG in the upper troposphere (200–500 hPa) over the eastern BOB (5°–15°N, 90°–100°E) in ENSO-decay years for all ENSO (Figure 1(a)), normal-decay ENSO (Figure 1(b)) and later-decay ENSO events (Figure 1(c)). As already identified in previous studies (Joseph *et al.*, 1994; Ju and Slingo, 1995; Chao and Chen, 2001; Mao and Wu, 2007; Liu *et al.*, 2015b), the reversal of the MTG over the BOB or the onset of the BOBSM is generally anomalously earlier/later

© 2017 Royal Meteorological Society

in cold/warm ENSO-decay years, when all moderately strong ENSO events are considered (Figure 1(a)). The average onset date of the BOBSM in warm ENSO years (pentad 26) is about three pentads later relative to that in cold ENSO years (pentad 23). However, when only the normal-decay ENSO events are considered, the timing of BOBSM onset does not change significantly between cold and warm ENSO years; the reversal of the MTG always lies in pentad 24 of the climatological mean date, though the MTG before its reversal in cold ENSO years is indeed slightly weaker than that in warm ENSO years (Figure 1(b)). This suggests that the contrasting BOBSM onset between warm and cold ENSO years may mainly be caused by those later-decay ENSO events. To prove this, we show the corresponding composite MTG evolutions for later-decay ENSO events in Figure 1(c). It is clear that the BOBSM onset dates change remarkably between warm and cold later-decay ENSO years. The much weaker MTG before BOBSM onset in cold ENSO years reverses as early as pentad 21–22, while the stronger MTG before BOBSM onset in warm ENSO years does not reverse until as late as pentad 26–27. Therefore, it can be concluded that the ENSO–BOBSM relationship identified by many previous studies is actually dominated by later-decay ENSO events, or the effect of ENSO would be largely insignificant without those ENSO events that decay far more slowly.

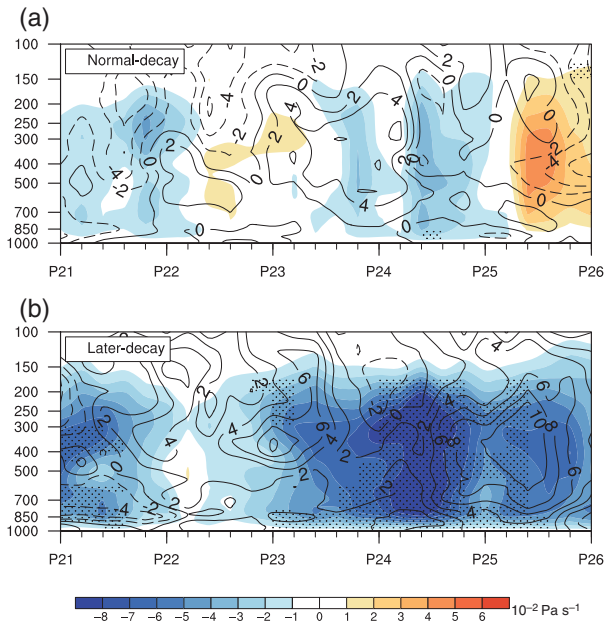

Figure 2. Daily evolutions (P21–26) of the cold-minus-warm composite vertical motion (Omega; shading; units: 10^{-2} Pa s^{-1}) and divergence (contours; units: 10^{-6} s^{-1}) anomalies over the northeastern BOB (10°–15°N, 90°–100°E) in (a) normal-decay and (b) later-decay ENSO years. Dotted areas indicate that the composite anomalies are statistically significant above the 90% confidence level according to the *t*-test.

4. Contrast in BOBSM onset processes between later-decay and normal-decay ENSO years

With regard to the generally symmetric responses to ENSO between warm and cold ENSO events, including those of the SST anomalies, atmospheric circulation and convection anomalies over the BOBSM region (Liu *et al.*, 2015b; Ren *et al.*, 2016), next we mainly use cold-minus-warm composite analysis to demonstrate ENSO's effects on BOBSM onset processes.

4.1. Contrasting vertical coupling of the circulation anomalies in troposphere

To understand the dominance of later-decay ENSO events in ENSO's influence on BOBSM, we first examine the changes in vertical coupling of circulation around the time of BOBSM onset due to the later-decay of ENSO events. Earlier studies have indicated a modulation by ENSO of the vertical coupling of circulation anomalies between the upper and lower troposphere during BOBSM onset (Liu *et al.*, 2015b). Figure 2 shows the cold-minus-warm composite daily evolutions of vertical motion anomalies and divergence anomalies over the northeastern BOB (10°–15°N, 90°–100°E) in normal-decay (Figure 2(a)) and later-decay (Figure 2(b)) ENSO years. It is obvious that, following normal-decay cold ENSO relative to warm ENSO, no significant upper-level divergence and mid-level vertical motion anomalies exist before the onset of the BOBSM. Anomalous ascent does not appear in the middle troposphere until late in pentad 23, which is generally the climatological mean time of BOBSM onset. In contrast, following later-decay cold ENSO relative to warm ENSO events, significant divergence anomalies in the upper troposphere begin to develop as early as the beginning of pentad 22, which is much earlier than the climatological mean time of the establishment of BOBSM convection (Figure 2(b)). Immediately after, significant ascent anomalies occur in the middle troposphere from the second day of pentad 22, which then grow rapidly and persist steadily (Figure 2(b)). This indicates the much earlier establishment of the vertical coupling of circulation anomalies between the upper and lower troposphere, that favours an earlier onset of BOBSM, due to the later-decaying of ENSO events. In addition, the slight temporal lead of the upper-level divergence over the mid-level ascent anomalies demonstrates the importance of the anomalous upper-level divergence-pumping effect for the development of BOBSM convection. Next we will diagnose the specific contrast of circulation anomalies respectively in the lower and upper troposphere.

4.2. Contrasting circulation anomalies in the lower troposphere

4.2.1. Climatological background

Previous studies have emphasized the importance of the establishment of the climatological India–Burma trough (Yin, 1949; Wu and Zhang, 1998; Kiguchi and Matsumoto, 2005; Chen, 2006; Liu and Ding, 2007), as well as the prevailing low-level converging flow over the Maritime Continent region (Zhang *et al.*, 1999; Wang *et al.*, 2000; Zhang

© 2017 Royal Meteorological Society

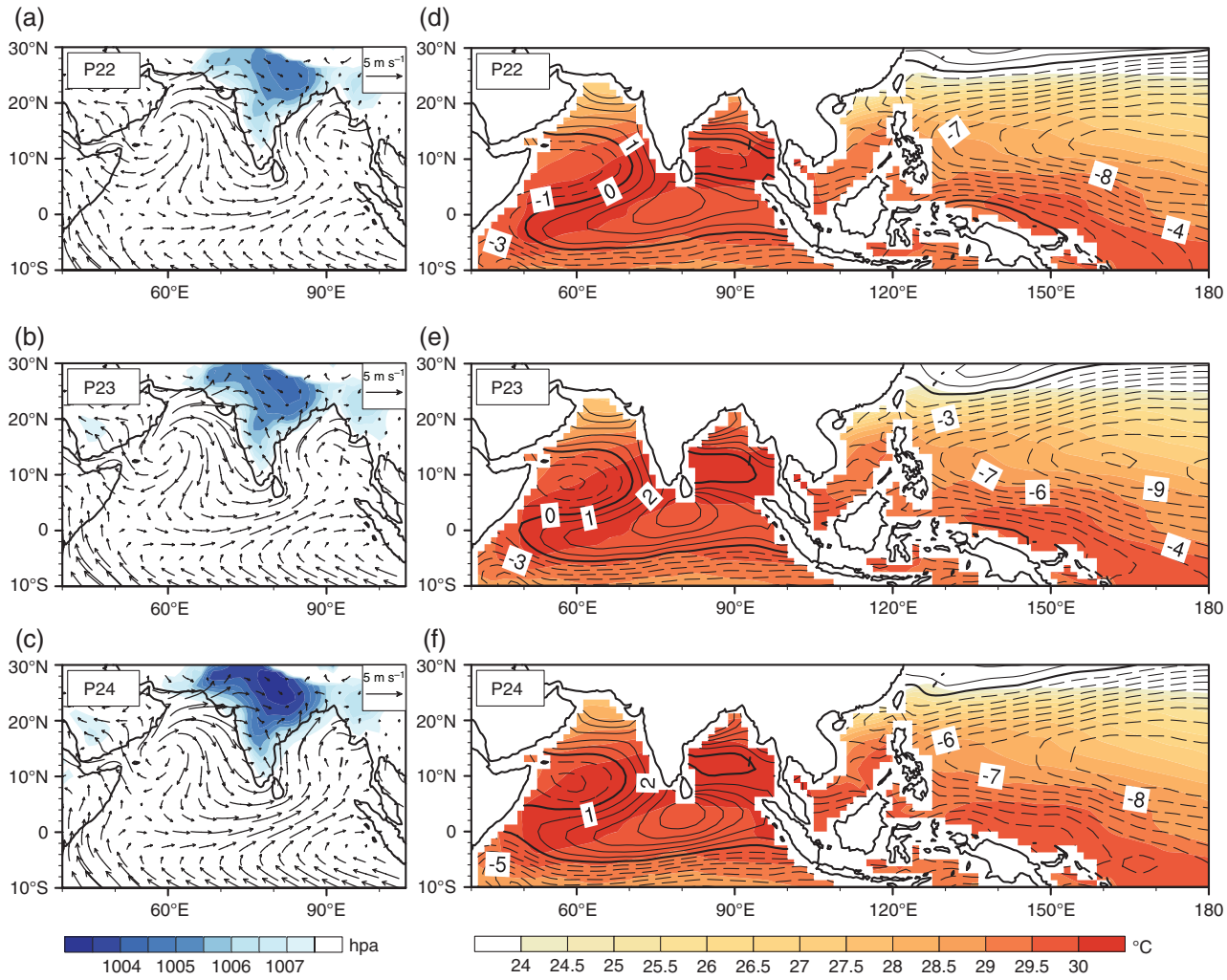

Figure 3. Climatology of (a–c) SLP (shading; units: hPa) and 10 m wind (vectors; units: m s^{-1}) and (d–f) SST (shading; units: °C) and 925 hPa zonal wind (contours; m s^{-1}) during BOBSM onset from pentad 22 to pentad 24 from 1958 to 2014.

and Sumi, 2002), for the onset of the BOBSM in April. To facilitate an understanding of the anomalous circulation in ENSO years, we first display in Figure 3 the climatological background low-level circulation patterns in pentads 22, 23 and 24, just prior to the climatological mean date of BOBSM onset, before our composite analysis. Clearly, the India–Burma trough has established in pentad 22 (Figure 3(a)), and it continues to deepen rapidly afterwards (Figures 3(b) and (c)). Thus, the surface southerlies ahead of the trough grow increasingly stronger over the BOB, which helps to move the tropical warmer and wetter air polewards to the west coast of the Indochina Peninsula. Meanwhile, the negative zonal gradient of SST over the Indo-Pacific region supports the prevailing easterlies over the western Pacific, and the northward cross-equatorial SST gradient over the Indian Ocean benefits the prevailing westerlies over the equatorial BOB during this period (Figures 3(d)–(f)); plus, they too increasingly gain in strength from pentad 22 to 24. The enhancing convergence over the Maritime Continent region thus favours the development of deep convection over the eastern BOB, or the onset of the BOBSM.

4.2.2. *Contrast between later-decay and normal-decay ENSO years*

Ren *et al.* (2016) indicated that the anomalous zonal Walker circulation in later-decay ENSO years is significantly stronger than that in normal-decay ENSO years, and can persist beyond the spring season into the summer months. The cold-minus-warm composite sea level pressure (SLP) and 10 m wind anomaly patterns during pentads 22, 23 and 24 (Figure 4) clearly indicate that, associated with the stronger and persistent ascending branch of the anomalous zonal Walker circulation over the tropical Indo-Pacific in later-decay cold ENSO years, the anomalous SLP low over the Indo-Pacific Ocean is also much stronger than that in normal-decay years (Figures 4(d)–(f) *vs* Figures 4(a)–(c)). While the negative SLP anomalies have diminished and even reversed over the western Indian Ocean prior to BOBSM onset in normal-decay cold ENSO years (Figures 4(a)–(c)), significant negative SLP anomalies persist over the IOB in later-decay cold ENSO years (Figures 4(d)–(f)). Correspondingly, while the surface wind anomalies become less significant during this period in normal-decay cold ENSO years

© 2017 Royal Meteorological Society

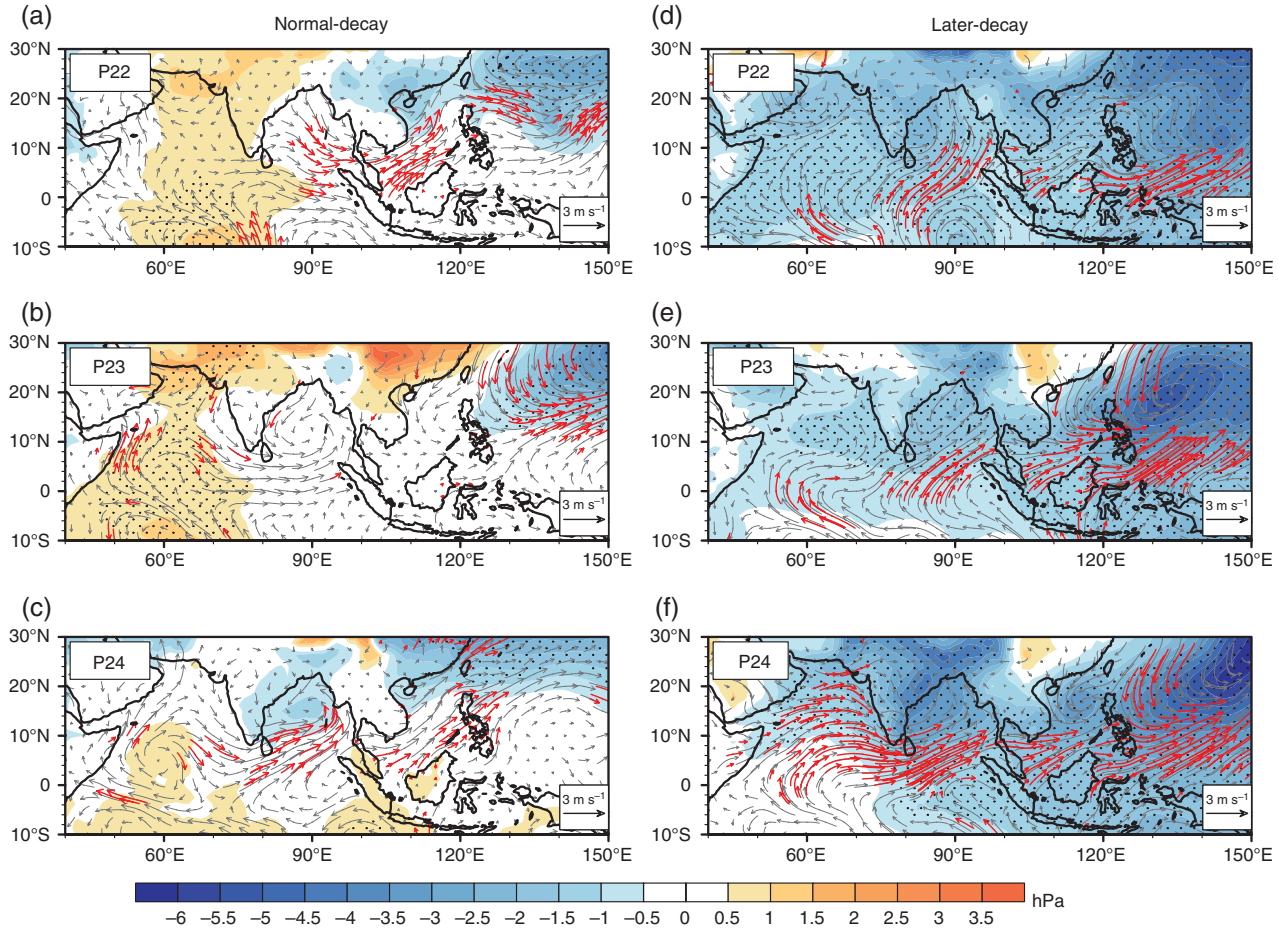

Figure 4. Cold-minus-warm composites of SLP anomalies (shading; units: hPa) and 10 m wind anomalies (vectors; units: m s^{-1}) during the BOBSM onset from pentad 22 to pentad 24 in (a–c) normal-decay and (d–f) later-decay ENSO years. Dotted and red vectors indicate that the composites are above the 90% confidence level according to the *t*-test.

(Figures 4(a)–(c)), significant southwesterly and westerly anomalies exist over the Indian Ocean in later-decay cold ENSO years (Figures 4(d)–(f)). The stronger negative SLP and the far more significant surface wind anomalies both favour an earlier establishment of the India–Burma trough, and possibly an earlier onset of the BOBSM.

In addition, previous studies have indicated that a BOB monsoon onset vortex (MOV) may also be an important signal leading to BOBSM onset (Wu *et al.*, 2011, 2012); and the necessary requirements for a MOV include existing barotropic instability induced by horizontal wind shear (Krishnamurti *et al.*, 1981) and proper boundary conditions associated with local SST (Gray, 1975, 1998; Joseph, 1990). It is apparent from Figure 4(b) that a cyclonic surface wind pattern does exist over the BOB in pentad 23 of normal-decay cold ENSO years, which may well be associated with an MOV at about 10°N (Lau *et al.*, 1998). It is worthwhile to note that in later-decay cold ENSO years, despite the basin-wide negative SST anomalies, which are supposed to block the organization of deep convection and the vortex, an anomalous surface cyclone actually forms before pentad 22 (not shown) and then triggers the significant westerly and southwesterly anomalies over the BOB (Figures 4(d)–(f)). This suggests an overwhelming dominance of barotropic instability processes (rather than the local underlying SST) for ENSO's influence on BOBSM onset in later-decay ENSO years.

To confirm the dominant effect caused by the wind-shear-induced barotropic instability, we first display the contrasts of the composite SST and zonal wind anomalies at 925 hPa from pentad 22 to pentad 24 in Figure 5. The weak cold SST anomalies over the BOB region correspond to westerly anomalies over the southern BOB in normal-decay cold ENSO years (Figures 5(a)–(c)); and the westerly centre grows slowly along the equator and shifts northward to 10°N until pentad 24 (Figure 5(c)). In contrast, in later-decay cold ENSO years, an intensifying positive zonal gradient of SST exists due to the significant negative SST anomalies over the BOB and the positive SST anomalies over the western Pacific (Figures 5(d)–(f)). Correspondingly, the anomalous 925-hPa westerlies over the BOB are much stronger than those in normal-decay ENSO years, and they expand northward to 10°N by pentad 23 in later-decay cold ENSO years (Figure 5(e)). These westerly anomalies, combined with the negative SLP anomalies over the northwestern Pacific (shown in Figures 4(d)–(f)), then contribute to an earlier onset of the BOBSM by enhancing the negative meridional

© 2017 Royal Meteorological Society

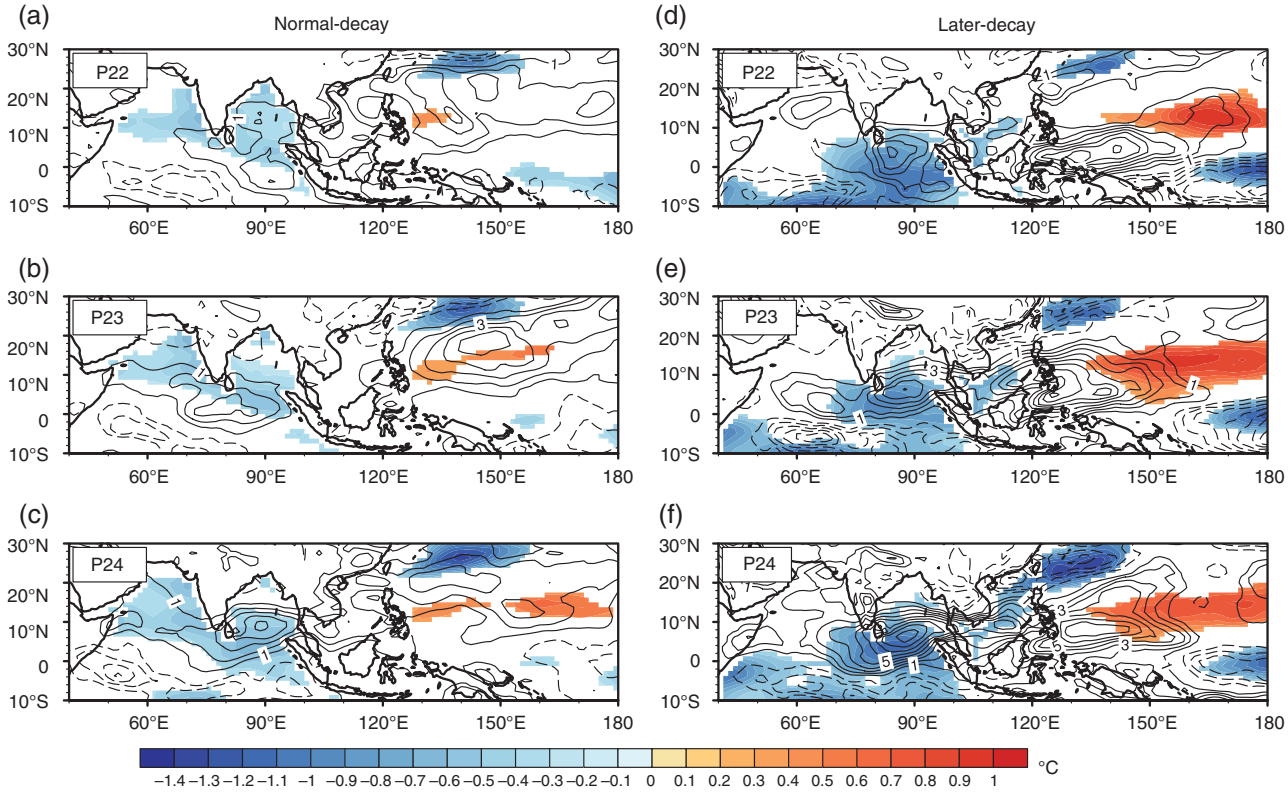

Figure 5. Cold-minus-warm composites of SST anomalies (shading; units: °C) and zonal wind anomalies at 925 hPa (contours; units: m s^{-1}) during BOBSM onset from pentad 22 to pentad 24 in (a–c) normal-decay and (d–f) later-decay ENSO years. Only those above the 90% confidence level are drawn.

shear of zonal wind or the barotropic instability over the northeastern BOB, and by bringing more water vapour into the BOB region (Krishnamurti *et al.*, 1981).

To further demonstrate the contrasting development of the anomalous westerlies and the related barotropic instability over the BOB in the lower troposphere between normal-decay and later-decay ENSO years, the pentad evolutions of the later-minus-normal composites of the area-mean zonal wind anomalies are presented for warm (Figure 6(b)) and cold (Figure 6(c)) ENSO-decay years. We follow Mao and Wu (2011) and Liu *et al.* (2015b) and average the zonal wind at 925 hPa over the region (70°–110°E) to represent the basic flow over the BOB. Firstly, the transition from easterly to westerly near 10°N always occurs around pentad 24 in normal-decay ENSO years, for both warm (Figure 6(b)) and cold (Figure 6(c)) ENSO events, coinciding with the climatological mean date of the reversal (Figure 6(a)). However, it is apparent from Figure 6(b) that, relative to normal-decay warm ENSO years, later-decay warm ENSO events act to suppress the establishment of the anomalous westerlies at 925 hPa by yielding generally out-of-phase anomalies during the onset of the BOBSM, and therefore the onset of the BOBSM itself. Conversely, by yielding significant westerly anomalies at 925 hPa around the time of BOBSM onset, later-decay cold ENSO events favour an earlier establishment of the anomalous westerlies from pentad 22 (Figure 6(c)), which can generate barotropic instability and facilitate the formation of a MOV over the northern BOB during the onset stage of the BOB summer monsoon.

To prove this, we display the temporal evolutions of the later-minus-normal composites of the meridional gradient of absolute vorticity [M] and the relative vorticity anomalies for warm (Figures 7(a) and (b)) and cold (Figures 7(c) and (d)) ENSO. Here the meridional gradient of absolute vorticity [M] is calculated following the method in Krishnamurti *et al.* (1981), to measure the wind-shear-induced barotropic instability,

$$[M] = -\frac{\partial^2}{\partial y^2}[u] + \beta \qquad (1)$$

where [u] denotes the BOB zonal basic flow (70°–110°E zonal-mean zonal wind as indicated above), β represents the meridional gradient of Coriolis parameter. Accompanying with the suppression of the anomalous westerlies in later-decay warm ENSO years relative to normal-decay years (Figure 6(b)), positive [M] anomalies is also suppressed over the southern BOB, leading to the same sign distribution of [M] over the south of 10°N during this period (Figure 7(a)). The unvaried sign of [M] over southern BOB indicates a mantaining condition of the local barotropic stability, which does not facilitate the formation of vortexes. As expected, significant anticyclonic vorticity anomalies prevail over BOB during pentads 23–28 (Figure 7(b)), helping to prevent the conditions for MOV generation in later-decay (relative to normal-decay) warm ENSO years. In contrast, in later-decay cold ENSO years,

© 2017 Royal Meteorological Society

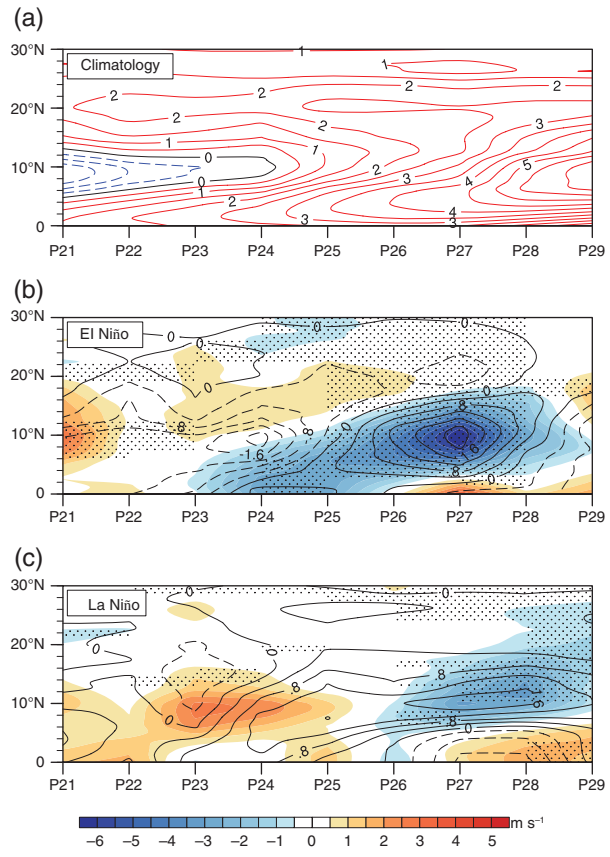

Figure 6. Pentad evolutions (P21–29) of (a) the climatological mean zonal wind and the later-minus-normal composite zonal wind anomalies (shading; units: m s^{-1}) at 925 hPa over the BOB (70°–110°E) during (b) warm and (c) cold ENSO-decay years. Contours in (b, c) represent the corresponding composite zonal wind anomalies for normal-decay ENSO years. Dotted and shaded areas indicate that the composite is statistically significant above the 90% confidence level according to the *t*-test.

corresponding to the significant westerly anomalies along the south side of 10°N (Figure 6(c)), the prevailing negative anomalies of meridional shear of zonal wind generate significant positive and negtive [*M*] anomalies respectively along the south and north flanks of 10°N from pentads 23 to 25 (Figure 7(c)). This marked alternation in the sign of [*M*] near 10°N denotes satisfied conditions for the existence of barotropic instablility, which correspondingly favours the cyclonic vorticity anomalies along the sign-reversal line of [*M*] near 10°N (Figure 7(d)) (just to the north of the anomalous westerlies in Figure 6(c)) during this period. The positive anomalous vorticity thus can facilitate the formation of MOV and trigger the earlier onset of BOBSM before the climatological mean onset date.

4.2.3. *Upper-tropospheric circulation*

Figure 8 presents the cold-minus-warm composites of the wind flow fields at 200 hPa (vectors) and diabatic apparent heat (Q_1) at 500 hPa for normal-decay (Figures 8(a)–(c)) and later-decay (Figures 8(d)–(f)) ENSO years. As we can see, whilst the composite differences in the anomalous circulation and diabatic Q_1 are largely insignificant between cold and warm events for normal-decay ENSO (Figures 8(a)–(c)), significant diabatic Q_1 anomalies exist over the southern SCS and Philippines during pentads 22–24 before the onset of the BOBSM following later-decay cold ENSO events relative to warm ENSO events (Figures 8(d)–(f)). And the diabatic Q_1 anomalies get enhanced over the eastern BOB associated with the significant ascending anomalies in the middle troposphere (shown in Figure 2). This condensation heating over BOB, which has been proved in a case study by Wu *et al.* (2005), is responsible for the reversal of mid-tropospheric MTG and the changes in large-scale circulation over South Asia. Coexisting with the significant diabatic Q_1 anomalies, an anomalous anticyclone appears to the north of the Indochina Peninsula, presenting as a Gill-type response to the diabatic heating (Gill, 1980). The anomalous diabatic heating and the anticyclone are the strongest in pentad 23 over the northeastern BOB (Figure 8(e)). By referring to the climatological background of upper-level troposphere, it is known that the SAH center first forms over the south of Indochina Peninsula in pentad 23, and then intensifies and extends to eastern BOB in pentad 24, centred at about 10°N (grean dashed circle in Figures 8(e) and (f)). Obviously, the anomalous anticyclone mentioned above lies to the north of SAH's climate-mean position, favouring a northwestward shift of the climatological SAH during the onset stage of the BOBSM in later-decay cold ENSO years relative to warm ENSO years. Therefore, the significant easterly anomalies to the south of the SAH, combined with the northeasterlies near the equator, form an anomalous divergence pattern (Figures 8(d)–(f)). This divergence pattern acts as an upper tropospheric pumping over the eastern BOB (Liu *et al.*, 2015b) to favour an earlier onset of the BOBSM, which is quite crucial for the establishment of a proper vertical coupling as indicated in Figure 2. This again indicates that ENSO's effect on the upper-tropospheric circulation over the BOB is primarily dominated by later-decay ENSO events.

5. Summary and discussion

Based on JRA-55 reanalysis and COBE SST data, this study demonstrates a close relationship between the seasonal timing of ENSO's decay phase and the onset of the BOBSM. By distinguishing later-decay events from normal-decay ENSO events, we first indicate that a later (earlier) onset of the BOBSM following warm (cold) ENSO events is actually caused mainly by those ENSO events that decay much slowly; and the ENSO–BOBSM relationship becomes insignificant when only the normal-decay ENSO events are considered. Diagnosis of the differences in circulation anomalies around BOBSM onset between later-decay and normal-decay ENSO years indicates that, due to the earlier decay of normal-decay ENSO and the earlier diminishment of the ENSO-induced atmospheric bridge processes over the Indo-Pacific region, the local SST and atmospheric circulation over the BOB are barely affected by either warm or cold normal-decay ENSO. Whereas, following later-decay

© 2017 Royal Meteorological Society

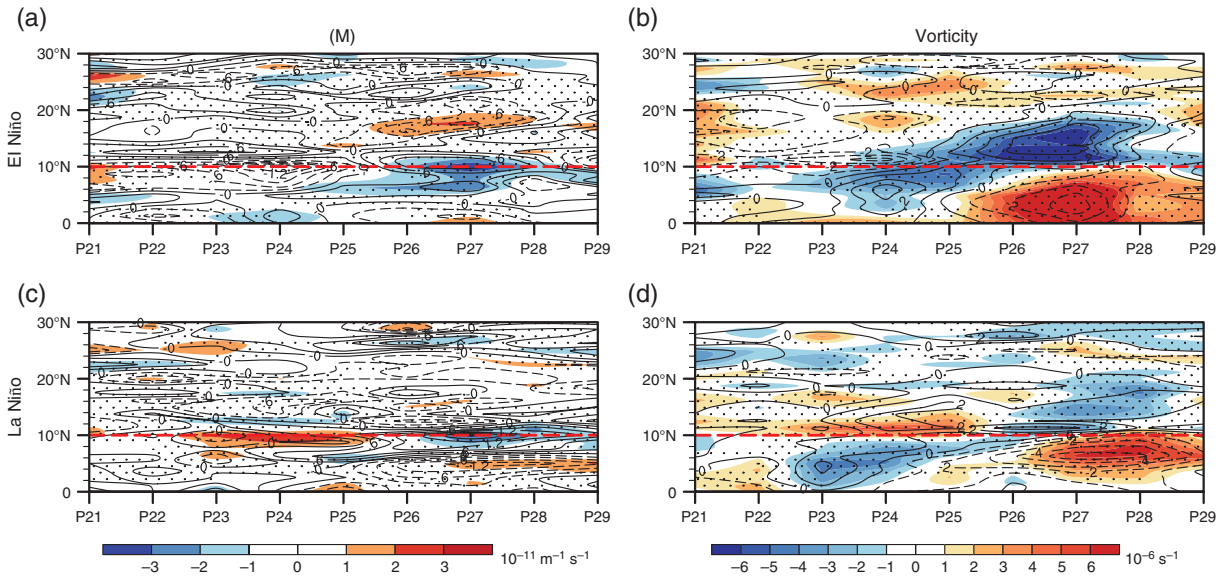

Figure 7. Pentad evolutions (P21–29) of the later-minus-normal composite (a, c) meridional gradient of absolute vorticity [M] (shading; units: 10^{-11} m^{-1} s^{-1}) and (b, d) relative vorticity (shading; units: 10^{-6} s^{-1}) at 925 hPa over the BOB (70°–110°E) during (a, b) warm and (c, d) cold ENSO-decay years. Contours represent the corresponding composite anomalies for normal-decay ENSO years. Dotted and shaded areas indicate that the composite is statistically significant above the 90% confidence level according to the t-test. Red dashed lines mark out the 10°N.

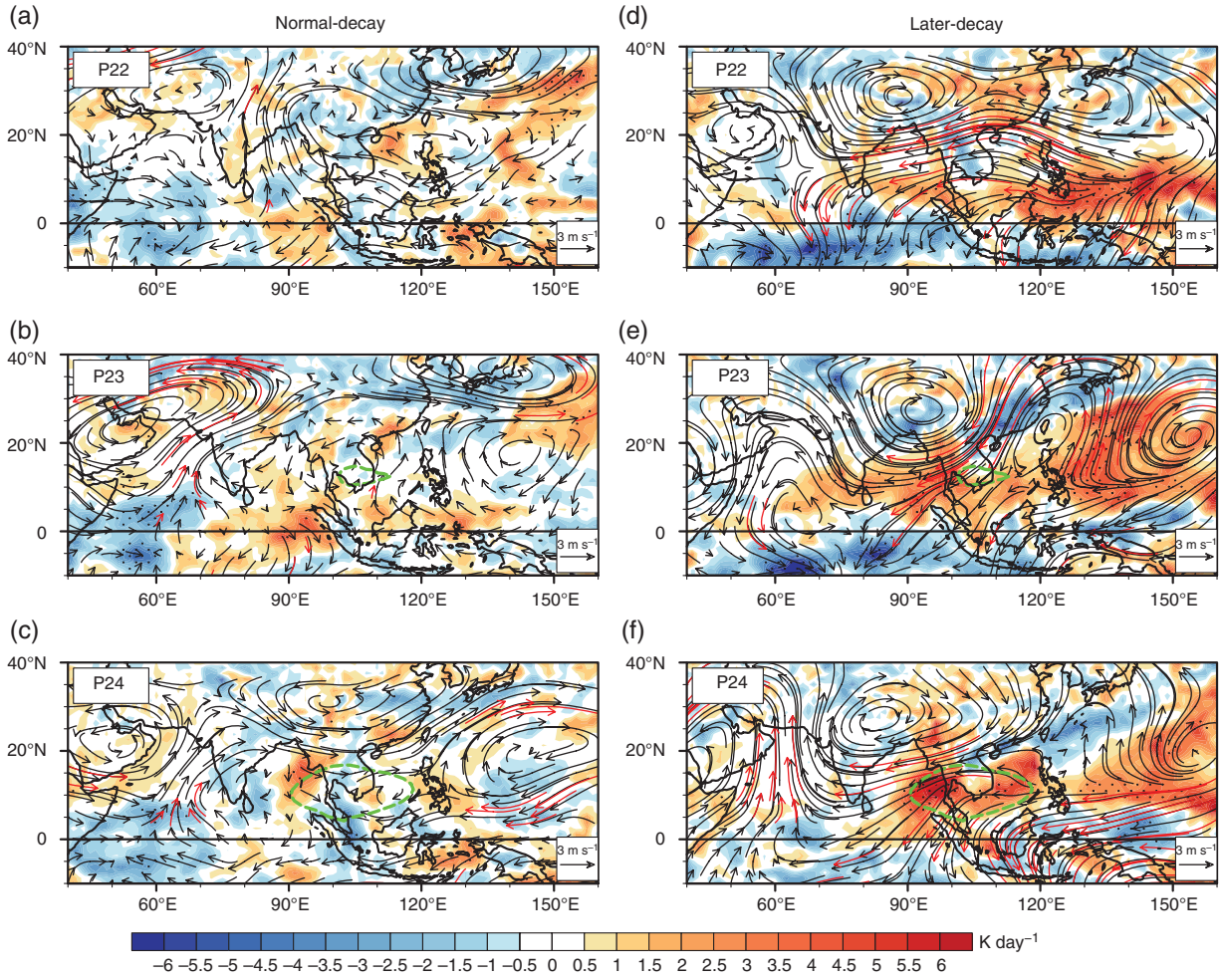

Figure 8. As in Figure 4, but for the composite 200-hPa streamline anomalies (vectors; units: m s^{-1}) and 500-hPa diabatic heating anomalies (shading; units: K day^{-1}). Dotted areas indicate the 90% confidence level of the composites according to the t-test. Green dashed circles mark the 12 460-gpm contour lines of geopotential height, which are used to represent the area coverage of the SAH closed-center.

© 2017 Royal Meteorological Society

ENSO events, the SST and atmospheric circulation over the BOB evolve in a contrasting fashion between warm and cold ENSO years, and thus the onset of the BOBSM is significantly modulated by later-decay ENSO events.

Specifically, following later-decay cold ENSO relative to warm ENSO, significant SST anomalies – being positive over the western Pacific but negative over the Indian Ocean and the central-eastern Pacific – are associated with westerly anomalies over the southern BOB and easterly anomalies over the western Pacific before BOBSM onset. In turn, the corresponding anomalous convergence over the Philippines supports the earlier development of local convection and diabatic heating, which stimulates an anomalous anticyclone in the upper troposphere and favours a northward shift of the SAH to the Indochina Peninsula. Thus, anomalous upper-level divergence can appear over the northeastern BOB before BOBSM onset. On the other hand, the persisting positive zonal gradient of SST between the Indian Ocean and the western Pacific along the equator also induces an earlier establishment of local westerly anomalies in the lower troposphere over the southern BOB, which are conducive to the earlier genesis of MOV mainly through enhancing the barotropic instability along 10°N over BOB, rather than because of the local SST conditons. Consequently, a significant early (later) onset of the BOBSM tends to occur following later-decay cold (warm) ENSO with the intensified (weakened) upper-level divergence-pumping, as well as the enhanced (reduced) lower-level barotropic instability.

In general, as the remote effects of ENSO on the Indo-Pacific region always lag ENSO by several months, a significant effect on the local SST and atmospheric circulation in this remote region therefore largely relies upon the speed at which ENSO events decay. The results of thhis study not only confirm ENSO's significant influence on the BOBSM but also indicate the importance of the seasonal timing of ENSO's decay phase for this remote influence. This helps us to understand the uncertainties in the ENSO–BOBSM relationship and will benefit the possibility of forecasting the onset of the BOBSM in the future. For the same reason, the influences of ENSO on other components of the ASM system, including the ISM, are also associated with the timing of ENSO's decay phase, which we will document in a separate paper on the contrasting onset processes for different summer monsoon systems.

Acknowledgements

This work was jointly supported by the National Science Foundation of China (NSFC, 41575041), a Chinese Academy of Sciences project (XDA11010402) and the other two NSFC projects (91437105, 41430533).

References

Alexander MA, Blade I, Newman M, Lanzante JR, Lau NC, Scott JD. 2002. The atmospheric bridge: the influence of ENSO teleconnections on air-sea interaction over the global oceans. *J. Clim.* **15**: 2205–2231.

Ananthakrishnan R, Soman MK. 1989. Onset dates of the southwest monsoon over Kerala for the period 1870–1900. *Int. J. Climatol.* **9**: 321–322.

Annamalai H, Liu P, Xie SP. 2005. Southwest Indian Ocean SST variability: its local effect and remote influence on Asian monsoons. *J. Clim.* **18**: 4150–4167.

Chao WC, Chen B. 2001. The origin of monsoons. *J. Atmos. Sci.* **58**: 3497–3507.

Chen Y. 2006. *A study of the southeast Asian summer monsoon onset, evolution and its influence on the weather and climate over the southwest of China (in Chinese)*. PhD dissertation, Nanjing University of Information Science and Technology, Nanjing, Jiangsu, China.

Chen L, Zhu Q, Luo H, He J, Dong M, Feng Z. 1991. *East Asian Monsoon*. Meteorological Press: Beijing, China, 362 pp (in Chinese).

Dee DP, Uppala SM, Simmons AJ, Berrisford P, Poli P, Kobayashi S, Andrae U, Balmaseda MA, Balsamo G, Bauer P, Bechtold P, Beljaars ACM, van de Berg L, Bidlot J, Bormann N, Delsol C, Dragani R, Fuentes M, Geer AJ, Haimberger L, Healy SB, Hersbach H, Holm EV, Lsaksen L, Kallberg P, Kohler M, Matricardi M, McNally AP, Monge-Sanz BM, Morcrette JJ, Park BK, Peubey C, deRosnay P, Tavolato C, Thepaut JN and Vitart F. 2011. The ERA-Interim reanalysis: configuration and performance of the data assimilation system. *Q. J. R. Meteorol. Soc.* **137**: 553–597.

Gill AE. 1980. Some simple solutions for heat-induced tropical circulation. *Q. J. R. Meteorol. Soc.* **106**: 447–462.

Gray WM. 1975. Tropical cyclone genesis. *Atmospheric science paper*, no. 234.

Gray WM. 1998. The formation of tropical cyclones. *Meteorog. Atmos. Phys.* **67**: 37–69.

Huang BH, Kinter JL. 2002. Interannual variability in the tropical Indian Ocean. *J. Geophys. Res-Oceans* **107**(C11): 3199. https://doi.org/10.1029/2001JC001278.

Ishii M, Shouji A, Sugimoto S, Matsumoto T. 2005. Objective analyses of sea-surface temperature and marine meteorological variables for the 20th century using icoads and the Kobe collection. *Int. J. Climatol.* **25**: 865–879.

Joseph PV. 1990. Warm pool over the Indian Ocean and monsoon onset. *Trop. Ocean-Atmos. Newslett.* **53**: 1–5.

Joseph PV, Eischeid JK, Pyle RJ. 1994. Interannual variability of the onset of the Indian-summer monsoon and its association with atmospheric features, El-Nino, and sea-surface temperature anomalies. *J. Clim.* **7**: 81–105.

Ju JH, Slingo J. 1995. The Asian summer monsoon and Enso. *Q. J. R. Meteorol. Soc.* **121**: 1133–1168.

Julian PR, Chervin RM. 1978. Study of southern oscillation and Walker circulation phenomenon. *Mon. Weather Rev.* **106**: 1433–1451.

Kiguchi M, Matsumoto J. 2005. The rainfall phenomena during the pre-monsoon period over the Indochina Peninsula in the GAME-IOP year, 1998. *J. Meteorol. Soc. Jpn.* **83**: 89–106.

Klein SA, Soden BJ, Lau NC. 1999. Remote sea surface temperature variations during ENSO: evidence for a tropical atmospheric bridge. *J. Clim.* **12**: 917–932.

Kobayashi S, Yukinari O, Yayoi H, Ayataka E, Masami M, Hirokatsu O, Kazutoshi O, Hirotaka K, Chiaki K, Hirokazu E, Kengo M, Kiyotoshi T. 2015. The JRA-55 Reanalysis: general specifications and basic characteristics. *J. Meteorol. Soc. Jpn Ser. II* **93**: 5–48.

Krishnamurti TN, Ardanuy P, Ramanathan Y, Pasch R. 1981. On the onset vortex of the summer monsoon. *Mon. Weather Rev.* **109**: 344–363.

Lau NC, Nath MJ. 1996. The role of the "atmospheric bridge" in linking tropical Pacific ENSO events to extratropical SST anomalies. *J. Clim.* **9**: 2036–2057.

Lau NC, Nath MJ. 2000. Impact of ENSO on the variability of the Asian-Australian monsoons as simulated in GCM experiments. *J. Clim.* **13**: 4287–4309.

Lau NC, Nath MJ. 2003. Atmosphere–ocean variations in the Indo-Pacific sector during ENSO episodes. *J. Clim.* **16**: 3–20.

Lau NC, Nath MJ. 2012. A model study of the air-sea interaction associated with the climatological aspects and interannual variability of the South Asian summer monsoon development. *J. Clim.* **25**: 839–857.

Lau KM, Yang S. 1997. Climatology and interannual variability of the southeast asian summer monsoon. *Adv. Atmos. Sci.* **14**: 141–162.

Lau KM, Wu HT, Yang S. 1998. Hydrologic processes associated with the first transition of the Asian summer monsoon: a pilot satellite study. *Bull. Am. Meteorol. Soc.* **79**: 1871–1882.

Li SL, Lu J, Huang G, Hu KM. 2008. Tropical Indian Ocean Basin Warming and East Asian summer monsoon: a multiple AGCM study. *J. Clim.* **21**: 6080–6088.

© 2017 Royal Meteorological Society

Li Q, Ren RC, Cai M, Wu GX. 2012. Attribution of the summer warming since 1970s in Indian Ocean Basin to the inter-decadal change in the seasonal timing of El Nino decay phase. *Geophys. Res. Lett.* **39**: L12702. https://doi.org/10.1029/2012GL052150.

Liu Y, Ding Y. 2007. Analysis of the basic features of the onset of Asian summer monsoon. *Acta Meteorol. Sin.* **65**: 511–526.

Liu Y, Ding Y. 2008. Teleconnection between the Indian summer monsoon onset and the Meiyu over the Yangtze River Valley. *Sci. China Ser. D Earth Sci.* **51**: 1021–1035.

Liu B, Liu Y, Wu G, Yan J, He J, Ren S. 2015a. Asian summer monsoon onset barrier and its formation mechanism. *Clim. Dyn.* **45**: 711–726

Liu BQ, Wu GX, Ren RC. 2015b. Influences of ENSO on the vertical coupling of atmospheric circulation during the onset of South Asian summer monsoon. *Clim. Dyn.* **45**: 1859–1875.

Mao J. 2001. *Variation in the configuration of subtropical anticyclone during seasonal transition and the Mechanism of Asian monsoon onset (in Chinese)*. PhD dissertation, Graduate University of Chinese Academy of Sciences, Beijing, China.

Mao J, Wu G. 2007. Interannual variability in the onset of the summer monsoon over the Eastern Bay of Bengal. *Theor. Appl. Climatol.* **89**: 155–170.

Mao J, Wu G. 2011. Barotropic process contributing to the formation and growth of tropical cyclone Nargis. *Adv. Atmos. Sci.* **28**: 483.

Mao J, Wu G, Liu Y. 2003. Study on the variation in the configuration of subtropical anticyclone and its mechanism during seasonal transition-part I: climatological features of subtropical high structure. *J. Meteorol. Res.* **17**: 274–286.

Mao JY, Chan JCL, Wu GX. 2004. Relationship between the onset of the South China Sea summer monsoon and the structure of the Asian subtropical anticyclone. *J. Meteorol. Soc. Jpn.* **82**: 845–859.

Masumoto Y, Meyers G. 1998. Forced Rossby waves in the southern tropical Indian Ocean. *J. Geophys. Res-Oceans* **103**: 27589–27602.

Oort AH, Yienger JJ. 1996. Observed interannual variability in the Hadley circulation and its connection to ENSO. *J. Clim.* **9**: 2751–2767.

Rayner NA, Parker DE, Horton EB, Folland CK, Alexander LV, Rowell DP, Kent EC and Kaplan A. 2003. Global analyses of sea surface temperature, sea ice, and night marine air temperature since the late nineteenth century. *J. Geophys. Res.-Atmos.* **108**(D14): 4407. https://doi.org/10.1029/2002JD002670.

Ren R, Sun S, Yang Y, Li Q. 2016. Summer SST anomalies in the Indian Ocean and the seasonal timing of ENSO decay phase. *Clim. Dyn.* **47**: 1827–1844. https://doi.org/10.1007/s00382-015-2935-0

Tao S, Chen L. 1987. A review of recent research on the East Asian summer monsoon in China. In *Monsoon Meteorology*, Chang C-P, Krishnamurti TN (eds). Oxford University Press: Hongkong, China.

Tokinaga H, Tanimoto Y. 2004. Seasonal transition of SST anomalies in the tropical Indian ocean during El Nino and Indian Ocean dipole years. *J. Meteorol. Soc. Jpn.* **82**: 1007–1018.

Wang B, LinHo . 2002. Rainy season of the Asian-Pacific summer monsoon. *J. Clim.* **15**: 386–398.

Wang B, Wu R. 1997. Peculiar temporal structure of the south china sea summer monsoon. *Adv. Atmos. Sci.* **14**: 177–194.

Wang B, Wu RG, Fu XH. 2000. Pacific-East Asian teleconnection: how does ENSO affect East Asian climate? *J. Clim.* **13**: 1517–1536.

Wang B, LinHo ZYS, Lu MM. 2004. Definition of South China Sea monsoon onset and commencement of the East Asia summer monsoon. *J. Clim.* **17**: 699–710.

Wang B, Huang F, Wu ZW, Yang J, Fu XH, Kikuchi K. 2009. Multi-scale climate variability of the South China Sea monsoon: a review. *Dyn. Atmos. Oceans* **47**: 15–37.

Webster PJ, Magana VO, Palmer TN, Shukla J, Tomas RA, Yanai M, Yasunari T. 1998. Monsoons: processes, predictability, and the prospects for prediction. *J. Geophys. Res-Oceans* **103**: 14451–14510.

Wu GX, Zhang YS. 1998. Tibetan Plateau forcing and the timing of the monsoon onset over South Asia and the South China Sea. *Mon. Weather Rev.* **126**: 913–927.

Wu C, Yang S, Wang A, Fong S. 2005. Effect of condensational heating over the Bay of Bengal on the onset of the South China Sea monsoon in 1998. *Meteorog. Atmos. Phys.* **90**: 37–47.

Wu GX, Guan Y, Wang TM, Liu YM, Yan JH, Mao JY. 2011. Vortex genesis over the Bay of Bengal in spring and its role in the onset of the Asian Summer Monsoon. *Sci. China-Earth Sci.* **54**: 1–9.

Wu GX, Guan Y, Liu YM, Yan JH, Mao JY. 2012. Air-sea interaction and formation of the Asian summer monsoon onset vortex over the Bay of Bengal. *Clim. Dyn.* **38**: 261–279.

Xie SP, Annamalai H, Schott FA, McCreary JP. 2002. Structure and mechanisms of South Indian Ocean climate variability. *J. Clim.* **15**: 864–878.

Xie SP, Hu KM, Hafner J, Tokinaga H, Du Y, Huang G, Sampe T. 2009. Indian Ocean capacitor effect on Indo-Western Pacific climate during the summer following El Nino. *J. Clim.* **22**: 730–747.

Yan J. 2005. *Asian summer monsoon onset and advancing process and the variation of the subtropical high (in Chinese)*. PhD dissertation, Graduate University of Chinese Academy of Sciences: Beijing, China.

Yang JL, Liu QY, Xie SP, Liu ZY, Wu LX. 2007. Impact of the Indian Ocean SST basin mode on the Asian summer monsoon. *Geophys. Res. Lett.* **34**(2): 155–164.

Yin MT. 1949. A synoptic-aerologic study of the onset of the summer monsoon over India and Burma. *J. Meteorol.* **6**: 393–400.

Yoo S-H, Yang S, Ho C-iH. 2006. Variability of the Indian Ocean sea surface temperature and its impacts on Asian-Australian monsoon climate. *J. Geophys. Res.-Atmos.* **111**(111): 630–637.

Yu WD, Xiang BQ, Liu L, Liu N. 2005. Understanding the origins of interannual thermocline variations in the tropical Indian Ocean. *Geophys. Res. Lett.* **32**(24): 275–279.

Yuan Y, Zhou W, Chan JCL, Li CY. 2008. Impacts of the basin-wide Indian Ocean SSTA on the South China Sea summer monsoon onset. *Int. J. Climatol.* **28**: 1579–1587.

Zhang RH, Sumi A. 2002. Moisture circulation over East Asia during El Nino episode in northern winter, spring and autumn. *J. Meteorol. Soc. Jpn.* **80**: 213–227.

Zhang RH, Sumi A, Kimoto M. 1999. A diagnostic study of the impact of El Nino on the precipitation in China. *Adv. Atmos. Sci.* **16**: 229–241.

© 2017 Royal Meteorological Society